연구논문

Journal of Drive and Control, Vol.13 No.4 pp.23-30 Dec. 2016
ISSN(print) 2234-8328 ISSN(online) 2287-6146
http://dx.doi.org/10.7839/ksfc.2016.13.4.023

Dynamic Modeling and Observer-based Servomechanism Control of a Towing Rope System

Anh Minh D. Tran and Young Bok Kim

Received: 07 Aug. 2016, Revised: 20 Sep. 2016, Accepted: 07 Nov. 2016

Key Words : Dynamic Modeling, Towing Rope System, Observer-based Servomechanism.

Abstract: This paper presents a control-oriented dynamical model of a towing rope system with variable-length. In this system, a winch driven by a motor's torque uses the towing rope to pull a cart. In general, it is a difficult and complicated process to obtain an accurate mathematical model for this system. In particular, if the rope length is varied by operating the winch, the varying rope dynamics needs to be considered, and the key physical parameters need to be re-identified... However, real time parameter identification requires long computation time for the control scheme, and hence undesirable control performance. Therefore, in this article, the rope is modeled as a straight massless segment, with the mass of rope being considered partly with that of the cart, and partly as halfway to the winch. In addition, the changing spring constant and damping constant of the towing rope are accounted for as part of the dynamics of the winch. Finally, a reduced-order observer-based servomechanism controller is designed for the system, and the performance is evaluated by computer simulation.

1. Introduction

Recently, cables have been used in many cable-actuated systems such as cable robots, elevators, cranes, towing vehicles, mine train transport systems, air-bone module-based wind energy units, mooring vessels, etc.[1-6] Fig. 1 illustrates some applications of cable-actuated systems. High acceleration maneuvers and higher payload to weight ratios are some of the advantages of exploiting cables. Therefore, there's been a lot of research in recently years into cable-actuated systems.

Although moving loads by means of cables is theoretically simple, it is fairly challenging to control the loads and cables since the cables used in cable-actuated systems are often flexible. In cable-driven robot applications, the cable is very light and stiff, so cable dynamics can be ignored[7,8]. However, in large-scale system, the mass and flexibility of the cables are significant and cannot be neglected. Among a lot of methods for modeling rope, lumped-mass method is often used. Milutinovic and Deur[9] introduced a multi body approach to obtain dynamic model of varying tether length. In this paper, the rope model includes a series of straight, massless, elastic segments with rope mass lumped to segment joints. And the numbers of unwound segments are changeable. This model accurately describes the catenary form of the rope and analyzes motion of the rope. However, the model is rather complex and it will be difficult to design the controller. According to Takeuchi and Liu[10], the elasticity of the long cable in the mine truck system

* Corresponding author: kpjiwoo@pknu.ac.kr
1 Department of Control & Mechanical Engineering, the Graduate School, Pukyong National University, Busan 608-739, Korea
2 Department of Mechanical System Engineering, Pukyong National University, Busan 608-739, Korea

creates vibration which is troublesome and reduces the efficiency of the convey system. Thus they construct a simplified 3-mass spring model with parameter perturbations. The system is nonlinear and time-varying because mass, spring constant and viscous friction depend on the position of the truck. So as to solve this problem, a time-invariant velocity controller is designed based on the rationally scaled control and simulation results show good performance. Further, Kang and Sul[11] suppressed the vibration for a lift car caused by the resonance of elastic ropes while the car is lifted. The rope mass is neglected but the changes of spring constant and damping constant of rope are examined. Extended full-order observer based on acceleration feedback compensation is derived and verified through the simulations and experiments. Nevertheless, these researches just focused on velocity and/or acceleration control.

This paper deals with the motion control of the cart driven by the towing rope system. The important issue includes developing a dynamic model of a towing rope system in which rope parameters depend on changing in length of rope.

In addition, it is considered the rope motion is difficult to measure. Therefore, a reduced-order observer is designed to estimate the motion states of the towing rope system[12]. Finally, the proposed method is proved by means of computer simulations.

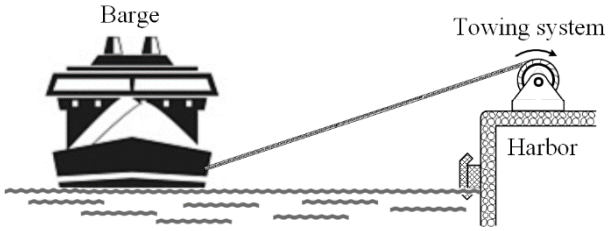

a) Ship berthing system

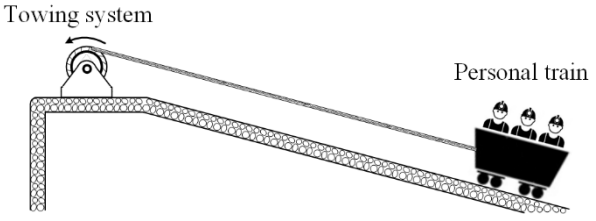

b) Mine train control system

Fig. 1 Applications of cable-actuated system

2. System modeling

2.1 Straight-line towing rope model

A straight segment is given as a model of the towing rope. This is shown in Fig. 2 in which a cart is connected to a winch through virtual mechanical components: a spring and a damper. Here, the spring constant and the damping constant characterize for the rope flexibility and are determined by change in length of towing rope. According to Moon et al.[13], spring constant and damping constant can be calculated as:

$$k_r = \frac{E_r A_r}{l_r} \tag{1}$$

$$b_r = \frac{B_r A_r}{l_r} \tag{2}$$

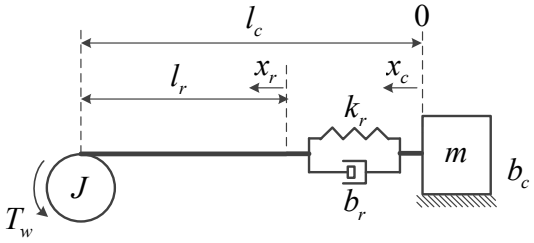

Fig. 2 Straight line rope model

The spread rope mass is lumped to two ends of the rope, in order that half of the rope mass is appended to the winch inertia and the other is added to the mass of the cart. So the total inertia moment on the winch and total mass on the cart are

$$m = m_c + \delta_r \frac{l_r}{2} \tag{3}$$

$$J = J_w + \frac{l_r}{2}\delta_r \left(r_w^2 + \frac{3}{4}r_r^2\right) \tag{4}$$

Where is the rope modulus of elasticity, is the rope cross section, is the rope constant damping, is the rope mass per meter, and are the radius of the winch and rope respectively.

As illustrated in Fig. 2, represents the variable length of the rope which is shortened when the winch winds

in and is the current (stretched) rope length, includes the natural (unstretched) rope length introduced above and the rope stretch created by the flexibility characteristics of the rope. Besides, is the position of the right end of the unstretched rope and is the position of the right end of the stretched rope which is also the position of the cart. The dynamical system equation can be expressed as:

$$\begin{cases} m\ddot{x}_c + b_c\dot{x}_c + k_r(x_c - x_r) + b_r(\dot{x}_c - \dot{x}_r) = 0 \\ J\dfrac{\ddot{x}_r}{r_w} + b_w\dfrac{\dot{x}_r}{r_w} + r_w k_r(x_r - x_c) + \\ \qquad r_w b_r(\dot{x}_r - \dot{x}_c) = T_w \end{cases} \tag{5}$$

$$\Rightarrow \begin{cases} \ddot{x}_c = \dfrac{k_r}{m}x_r + \dfrac{b_r}{m}\dot{x}_r - \dfrac{k_r}{m}x_c - \dfrac{b_r + b_c}{m}\dot{x}_c \\ \ddot{x}_r = -\dfrac{r_w^2 k_r}{J}x_r - \dfrac{r_w^2 b_r + b_w}{J}\dot{x}_r + \dfrac{r_w^2 k_r}{J}x_c \\ \qquad + \dfrac{r_w^2 b_r}{J}\dot{x}_c + \dfrac{r_w}{J}T_w \end{cases} \tag{6}$$

where is the input torque of the winch motor, is the rotational viscous coefficient caused by wire tension and friction force of the winch spindle and bearing, and is the friction between the cart and the plane. Finally, the state-space equation for motion of the cart driven by towing rope system can be derived

$$\begin{cases} \dot{x} = Ax + Bu \\ y = Cx \end{cases} \tag{7}$$

$$x = [x_1\ x_2\ x_3\ x_4]^T = [x_r\ \dot{x}_r\ x_c\ \dot{x}_c]^T$$
$$y = x_1$$
$$u = T_w$$

Where,

$$A = \begin{bmatrix} 0 & 1 & 0 & 0 \\ -\dfrac{r_w^2 k_r}{J} & -\dfrac{r_w^2 b_r + b_w}{J} & \dfrac{r_w^2 k_r}{J} & \dfrac{r_w^2 b_r}{J} \\ 0 & 0 & 0 & 1 \\ \dfrac{k_r}{m} & \dfrac{b_r}{m} & -\dfrac{k_r}{m} & -\dfrac{b_r + b_c}{m} \end{bmatrix}$$

$$B = \begin{bmatrix} 0 & \dfrac{r_w}{J} & 0 & 0 \end{bmatrix}^T$$

$$C = [1\ \ 0\ \ 0\ \ 0]$$

2.2 Simplified model for the towing rope system

As the winch winds in to maneuver the cart, the length of rope changes which varies the values of the total inertia moment of the winch, the total mass on the cart, the damping constant and spring constant on the towing rope. These parameters are analyzed with assumption that the length of rope varies from 2m to 20m and using the simulation parameters in S. M. Moon et al.[13] summarized in Table 1.

Table 1 Towing rope system parameters[13]

Item	Parameter	Value	Unit
Winch			
Radius		0.085	m
Width		0.22	m
Density steel		8000	kg/m^3
Inertia moment		0.095	kg·m^2
Viscous coefficient		50	N·m·s/rad
Wire rope			
Cross section area		47x10^{-6}	m^2
Elasticity modulus		193x10^9	Pa
Constant of damping		5.2x10^9	Pa·s
Total rope length		20	m
Radius		0.0039	m
Mass per meter		0.2388	kg/m
Cart			
Mass		300	kg
Viscous friction		3000	N·s/m

As can be seen in Fig. 3, the spring constant and the damping constant of the rope change a lot when the rope length changes. But the total inertia moment on the winch and the total mass on the cart vary a little. Thus lumped mass of rope on the winch and the cart can be eliminated; the state space equation of the system can be simplified and expressed as

$$\begin{cases} \dot{x} = Ax + Bu \\ y = Cx \end{cases} \quad \text{with} \tag{8}$$

$$A = \begin{bmatrix} 0 & 1 & 0 & 0 \\ -\dfrac{r_w^2 k_r}{J_w} & -\dfrac{r_w^2 b_r + b_w}{J_w} & \dfrac{r_w^2 k_r}{J_w} & \dfrac{r_w^2 b_r}{J_w} \\ 0 & 0 & 0 & 1 \\ \dfrac{k_r}{m_c} & \dfrac{b_r}{m_c} & -\dfrac{k_r}{m_c} & -\dfrac{b_r + b_c}{m_c} \end{bmatrix}$$

$$B = \begin{bmatrix} 0 & \dfrac{r_w}{J_w} & 0 & 0 \end{bmatrix}^T$$

$$C = [1\ \ 0\ \ 0\ \ 0]$$

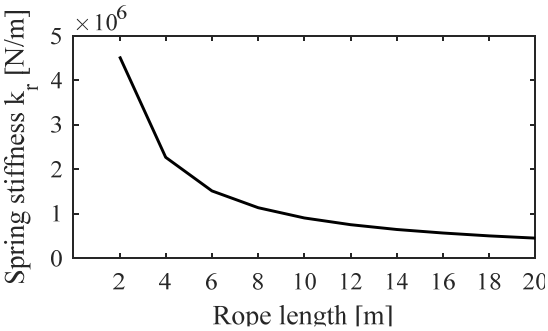

(a) Rope length vs. spring stiffness

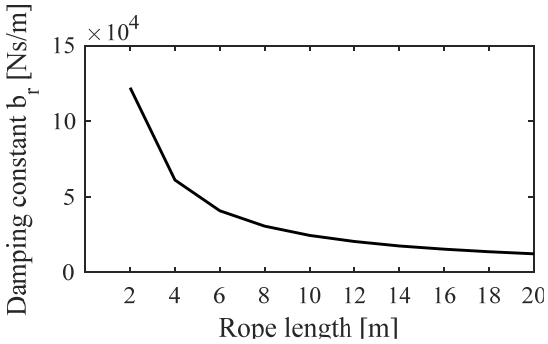

(b) Rope length vs. damping constant

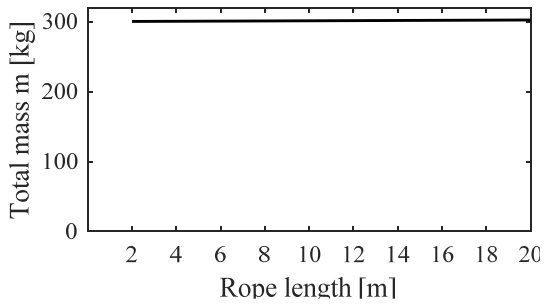

(c) Rope length vs. total mass

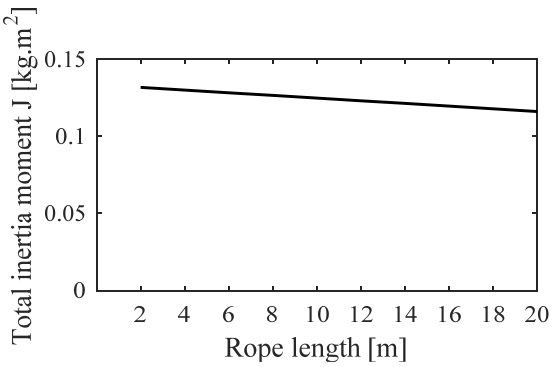

(d) Rope length vs. total inertia moment

Fig. 3 Parameter variations of towing rope system

Fig. 4 shows the frequency response of the towing rope system with varying length.

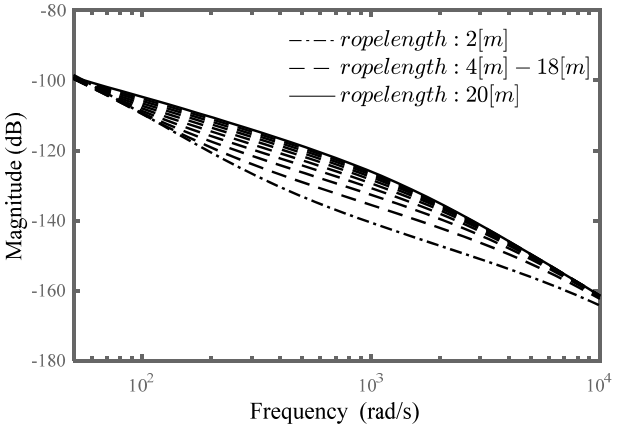

Fig. 4 Bode plot of the rope length parameter-dependent towing rope system.

In addition, an impulse response of open-loop system is implemented to verify the reduced model of towing rope system. As shown in Fig. 5, after applying input torque, the winch rotates and winds in rope, the unstretched rope length is shortened, however the length of the stretched rope differs with the length of the unstretched rope. This mismatch appears due to the flexibility characteristics of the towing rope.

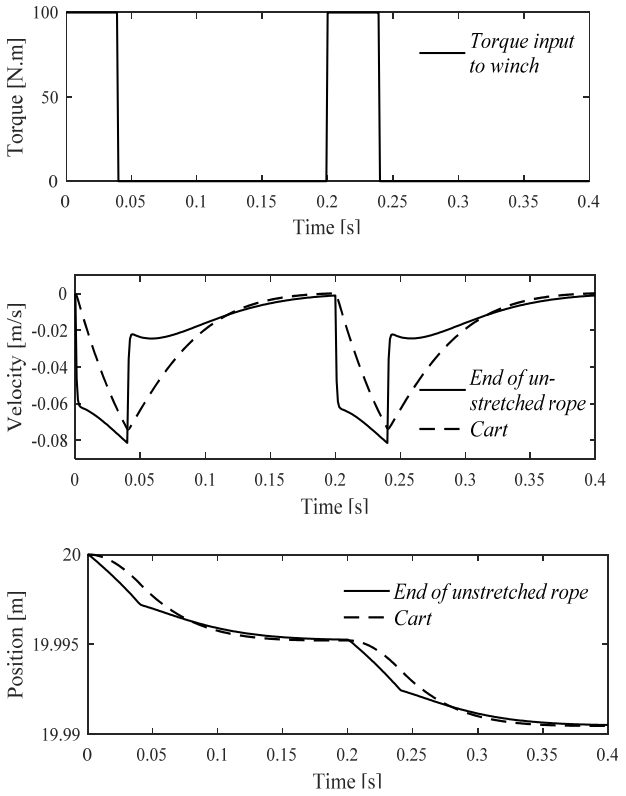

Fig. 5 Impulse response of towing rope system (open-loop)

3. Reduced-order observer based controller design and simulation result

In order to precisely control the motion and obtain zero steady-state error in the towing rope system, a servomechanism design methodology[14] (Ogata, 2002) is applied. Furthermore, a reduced-order observer[15] (Levine, 1996) is designed to estimate the states because it is considered difficult to measure the rope motion states.

The open-loop towing rope system described in Eq. (8) can be partitioned as follows

$$\begin{cases} \dot{x} = \begin{bmatrix} A_{11} & A_{12} \\ A_{21} & A_{22} \end{bmatrix} x + \begin{bmatrix} B_1 \\ B_2 \end{bmatrix} u \\ y = Cx \end{cases} \tag{9}$$

with

$$A_{11} = 0$$

$$A_{12} = [1 \quad 0 \quad 0]$$

$$A_{21} = \begin{bmatrix} -\frac{r_w^2 k_r}{J_w} & 0 & \frac{k_r}{m_c} \end{bmatrix}^T$$

$$A_{22} = \begin{bmatrix} -\frac{r_w^2 b_r + b_w}{J_w} & \frac{r_w^2 k_r}{J_w} & \frac{r_w^2 b_r}{J_w} \\ 0 & 0 & 1 \\ \frac{b_r}{m_c} & -\frac{k_r}{m_c} & -\frac{b_r + b_c}{m_c} \end{bmatrix}$$

$$B_1 = 0$$

$$B_2 = \begin{bmatrix} \frac{r_w}{J_w} & 0 & 0 \end{bmatrix}^T$$

$$C = [1 \quad 0 \quad 0 \quad 0]$$

The state vector in is separated into two sub-states to make the description of the reduced-order observer simplifier

$$x = [x_a \quad x_b^T] \tag{10}$$

such that

$$x_a = x_1 = y = Cx \tag{11}$$

is the measurement vector and

$$x_b = [x_2 \quad x_3 \quad x_4]^T \tag{12}$$

contains the components of the state vector that cannot be measured directly. Regarding and the plant dynamics can be written as

$$\begin{aligned} \dot{x}_a &= A_{11} x_a + A_{12} x_b + B_1 u \\ \dot{x}_b &= A_{21} x_b + A_{22} x_b + B_2 u \end{aligned} \tag{13}$$

There is no need to design observer for because is directly measured

$$\hat{x}_a = x_a = x_1 = y \tag{14}$$

We define the reduced-order observer for the remaining sub-state instead

$$\hat{x}_b = Ky + z \tag{15}$$

where is the state of a system of order 3

$$\dot{z} = \hat{A}\hat{x}_b + \bar{L}y + Hu \tag{16}$$

Fig. 6 shows the block diagram of the reduced-order observer. The matrices and are chosen to ensure that the error in the estimation of the state converges to zero, independent of and.

$$\begin{aligned} \hat{A} &= A_{22} - KA_{12} \\ \bar{L} &= A_{21} - KA_{11} \\ H &= B_2 - KB_1 \end{aligned} \tag{17}$$

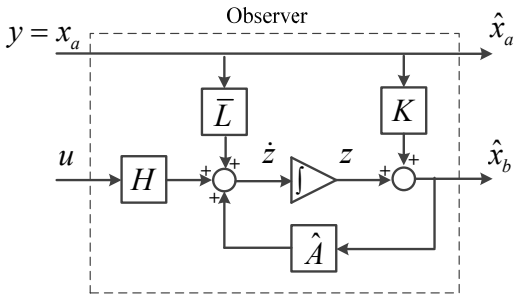

Fig. 6 A reduced-order observer

The servomechanism reduced-order observer-based compensator is of the form

$$\begin{aligned} \dot{x} &= (A - BF_c)x + BF_i x_i + BF_{c2} e_b \\ \dot{x}_i &= r - y \\ \dot{e}_b &= (A_{22} - KA_{12}) e_b \end{aligned} \tag{18}$$

where is the reference signal; is the error vector in estimation of, is the state feedback gain vector and is the augmented feedback gain.

These equations can be repackaged as

$$\begin{bmatrix}\dot{x}\\ \dot{x}_i\\ \dot{e}_b\end{bmatrix}=\begin{bmatrix}A-BF_c & BF_i & BF_{c2}\\ -C & 0 & 0\\ 0 & 0 & A_{22}-KA_{12}\end{bmatrix}\begin{bmatrix}x\\ x_i\\ e_b\end{bmatrix}+\begin{bmatrix}0\\ 1\\ 0\end{bmatrix}r \quad (19)$$

The observer-based servomechanism block diagram is shown in Fig. 7.

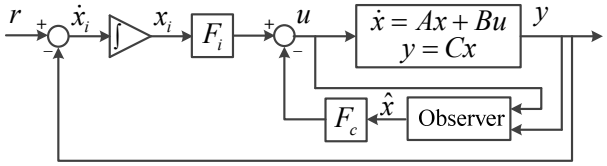

Fig. 7 Observer-based servomechanism block diagram.

In this paper, pole placement technique is used to determine the feedback gain matrix and the estimator gain matrix.

Control eigenvalues are chosen as

$$\lambda_c=[-53.7 \quad -59.1 \quad -64.4 \quad -69.8 \quad -75.2]$$

and this yields the augmented state feedback gain vector

$$[F_c \quad -F_i] = [-389380 \quad -11086 \quad 393590 \quad 10584 \quad -82399] \quad (20)$$

And observer eigenvalues are chosen as

$$\lambda_o=[-805 \quad -1611 \quad -2416]$$

and this gives the observer gain vector

$$K=[-5040 \quad -319 \quad 12841]^T \quad (21)$$

Simulations with spring and damping parameters varying regarding the length of rope are implemented to evaluate the proposed controller. The results which simulate the towing rope system pulling the cart are shown in Fig. 8 All cases show desirable position tracking performance.

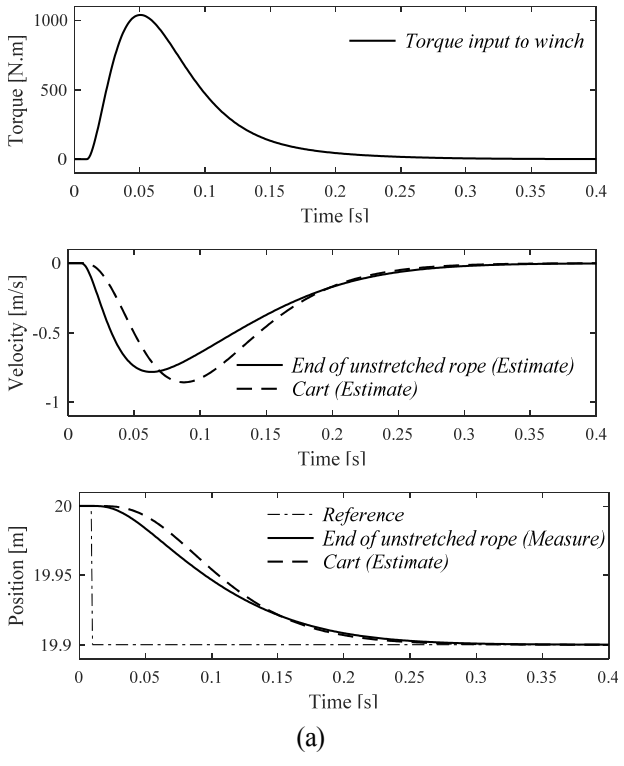

Fig. 8 Simulation plots of proposed reduced-order observer servomechanism control. From top to bottom: input torque to winch; velocity of unstretched rope ($\dot{x}_r$) and cart ($\dot{x}_c$); position of unstretched rope (x_r) and cart (x_c). (a) 20m rope length. (b) 2m rope length.

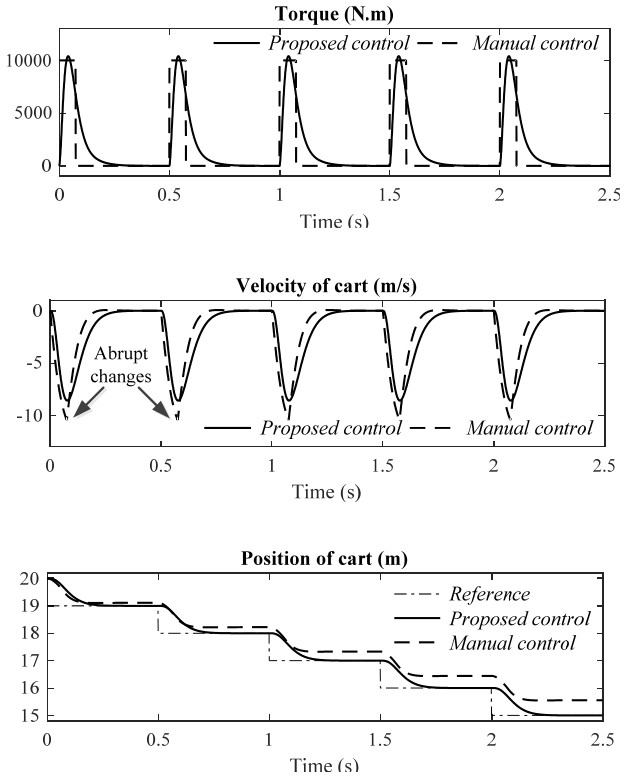

Fig. 9 Comparison plots of proposed control method and manual control cases.

Another simulation is carried out to check the efficiency of the controller. Here responses of the proposed control method and manual control cases are compared. As demonstrated in Fig. 9, the velocity of cart changes smoothly and the cart can track the reference position when using the proposed control method. In the manual control case, velocity of cart alters quickly, the abrupt changes appear and the cart cannot follow the reference input. This result shows the effects of the proposed controller.

4. Conclusions

This study has examined a control-oriented dynamic model of a towing rope system with variable-length. By looking upon varying spring and damping constants of rope, the changing length of the rope is more accurately modeled. After that a reduced-order observer-based servomechanism controller is designed using pole placement technique to track the desired motion. It is verified through simulations that the proposed model is effective.

Acknowledgement

This work was supported by the National Research Foundation of Korea (NRF) grant funded by the Korea Government (Ministry of Education) (No.NRF-2015 R1D1A1A09056885).

References

1) J. J. Gorman, K. W. Jablokow, and D. J. Cannon, “The cable array robot: Theory and experiment” Proceedings of the 2001 IEEE International Conference on Robotics and Automation, pp. 2804-2810, 2001.
2) K. Nai, W. Forsythe and R. M. Goodall, “Vibration Reduction Techniques for High Speed Passenger Elevators”, Proceedings of the Third IEEE Conference on Control Applications, Glasgow, Vol. 2, pp. 965-970, 1994.
3) E. Imanishi, T. Nanjo and T. Kobayashi, “Dynamic simulation of wire rope with contact”, Journal of Mechanical Science and Technology, Vol. 23, pp. 1083-1088, 2009
4) S. Ouchi, K. Z. Liu, S. Sato and T. Mita, “Mine Train Control System by Control”, Transactions of the Society of Instrument and Control Engineers, Vol. 34 , No. 3, pp. 225-231, 1998.
5) A. Cherubinia, A. Papinia, R. Vertechyb and M. Fontana, “Airborne Wind Energy Systems: A review of the technologies”, Renewable and Sustainable Energy Reviews, Vol. 51, pp. 1461-1476, 2015.
6) J. P. Strand, A. J. Sørensen and T. I. Fossen, “Design of Automatic Thruster Assisted Position Mooring Systems for Ships”, Modeling, Identification and Control, Vol. 19, No. 2, pp.61-75, 1998.
7) S. R. Oh and S. K. Agrawal, “Generation of feasible set points and control of a cable robot,” IEEE Transactions on Robotics, Vol. 22, No. 3, pp. 551-558, 2006.
8) D. Lau, D. Oetomo, and S. K. Halgamuge, “Generalized modeling of multilink cable-driven

manipulators with arbitrary routing using the cable routing matrix", Transactions on Robotics, Vol. 29, No. 5, pp. 1102-1113, 2013.

9) M. Milutinovic, N. Kranjcevic and J. Deur, "Multi-mass dynamic model of a variable-length tether used in a high altitude wind energy system", Energy Conversion and Management, Vol. 87, 1141:1150, 2014.

10) H. Takeuchi, K. Liu and S. Ouchi, "Velocity Control of a Mine Truck System using Rationally Scaled Control", Proceedings of the 35th IEEE Conference on Decision and Control, pp. 767-772, 1996.

11) J. K. Kang and S. K. Sul, "Vibration Control of Elevator Using Estimated Car Acceleration Feedback Compensation", IEEE Transactions on Industrial Electronics, Vol. 47, No. 1, pp. 91-99, 2000.

12) R. L. Williams II and D. A. Lawrence, "Linear State-Space Control Systems", John Wiley & Sons, Hoboken, NJ, 2007.

13) S. M. Moon, J. Huh, D. Hong, S. Lee and C.S. Han, "Vertical motion control of building facade maintenance robot with built-in guide rail", Robotics and Computer-Integrated Manufacturing, pp. 11-20, 2015.

14) K. Ogata, Modern Control Engineering, 4th ed., Prentice Hall, Upper Saddle River, NJ, 2002.

15) W. S. Levine, The Control Handbook, Vol. 1, CRC Press, Boca Raton, FL, 1996.